

Advancement of extreme environment additively manufactured alloys for next generation space propulsion applications



Paul Gradl^{a,*}, Omar R. Mireles^a, Colton Katsarelis^b, Timothy M. Smith^d, Jeff Sowards^b, Alison Park^c, Poshou Chen^e, Darren C. Tinker^a, Christopher Protz^b, Tom Teasley^a, David L. Ellis^d, Christopher Kantzos^d

^a Propulsion Department, NASA Marshall Space Flight Center, Huntsville, AL, 35812, USA

^b Materials and Processes Laboratory, NASA Marshall Space Flight Center, Huntsville, AL, 35812, USA

^c NASA Engineering and Safety Center, NASA Langley Research Center, Hampton, VA, 23666, USA

^d High Temperature and Smart Alloy Branch, NASA Glenn Research Center, Cleveland, OH, 44135, USA

^e Jacobs ESSCA Group, NASA Marshall Space Flight Center, Huntsville, AL, 35812, USA

ARTICLE INFO

Keywords:

Additive manufacturing
 Propulsion
 Rockets
 Alloy development
 GRCop-42
 GRCop-84
 Refractory
 GRX-810
 NASA HR-1
 L-PBF
 LP-DED
 DED
 Laser powder bed fusion
 Laser powder directed energy deposition

ABSTRACT

The National Aeronautics and Space Administration (NASA) has been involved in the development and maturation of metal additive manufacturing (AM) for space applications since the late 2000's. Several efforts have focused on the understanding of AM processes through material characterization and testing, standards development, component fabrication, and infusion into propulsion development and flight applications. NASA matured commonly used aerospace alloys from various alloy families (Nickel, Copper, Stainless and Steel, Aluminum, and Titanium-based) through detailed AM process and heat treatment characterization, in addition to mechanical and thermophysical testing. While these alloys are actively used in many propulsion applications, there is a need for ongoing AM optimized alloys using integrated computational materials engineering (ICME) and process development for high performance applications. The applications targeted are liquid rocket engines; advanced propulsion systems; and in-space propulsion with high heat fluxes, high pressure, and/or that use propellants that can degrade alloys (e.g., hydrogen). This paper highlights the characterization and physical properties of the more common AM alloys using laser powder bed fusion (L-PBF) and laser powder directed energy deposition (LP-DED) processes. Additionally, this paper discusses some of the ongoing novel alloy development and maturation using AM for use in these harsh environments, such as GRCop-42, GRCop-84, NASA HR-1, GRX-810, and C-103. The results from these processes demonstrated that AM could enable rapid development, and that optimized alloys could be developed using ICME, yielding higher performances. These alloys have undergone modeling, fundamental metallurgical evaluations, heat treatment studies, detailed microstructure characterization, and mechanical testing campaigns. This, combined with direct application-specific component fabrication and hot-fire testing, enabled the increase of the Technology Readiness Level (TRL) through high duty-cycle testing. A background and overview of these novel AM-enabled alloys and AM processing developments including metallurgical and mechanical property studies is presented here. The latest advancement in the parallel component development and hot-fire testing and future developments for these alloys is also discussed.

1. Introduction

Material selection for an end-use aerospace application is critical for both component and mission success. Aerospace propulsion components provide unique challenges due to the demanding end-use environments in addition to programmatic and system requirements to meet mass,

economics, and acceptable risk [1]. The appropriate selection, utilization of metal alloys, and their processing throughout the entire component life cycle have a substantial impact on the success of the components once they are put into service. [2]. Propulsion components are typically designed with minimal margins to reduce mass, so a thorough understanding of the material behavior under the expected operating conditions and environment is critical. While various

* Corresponding author.

E-mail address: Paul.R.Gradl@nasa.gov (P. Gradl).

Acronyms/Abbreviations	
AM	Additive Manufacturing
CDS	Carbide Dispersion Strengthened
DED	Directed Energy Deposition
DOD or FOD	Domestic or Foreign Object Debris
HEE	Hydrogen Environment Embrittlement
HEI	Hydrogen Embrittlement Index
HIP	Hot Isostatic Pressing
ICME	Integrated Computational Materials Engineering
LCF	Low Cycle Fatigue
L-PBF	Laser Powder Bed Fusion
LP-DED	Laser Directed Energy Deposition
LRE	Liquid Rocket Engine
MTD	Manufacturing Technology Demonstrator
NASA	National Aeronautics and Space Administration
NTP	Nuclear Thermal Propulsion
ODS	Oxide Dispersion Strengthened
PBF	Powder Bed Fusion
RCS	Reaction Control System
RHEA	Refractory High Entropy Alloys
TRL	Technology Readiness Level
UTS	Ultimate Tensile Strength

materials are used for propulsion components, metals and metal alloys are the most common. They often come from alloy families including aluminum-, stainless steel, titanium-, nickel- and iron-based superalloys, copper-, refractory-, and platinum-based alloys [3].

The metals and metal alloys used for propulsion applications must meet a long list of technical requirements in addition to satisfying programmatic goals. These requirements often include high strength-to-weight ratios, capacity to operate cyclical and sustained static and dynamic loads (i.e., long-life duty cycles), chemical compatibility with fuels and/or oxidizers, the ability to withstand both cryogenic (-253°C) and elevated temperatures (often $>1000^{\circ}\text{C}$), and to have thermal expansion coefficients equivalent to alloys to which they are mated or joined. These requirements stem from harsh operating of modern liquid rocket engines where chamber temperatures can exceed 3300°C and where the chamber and coolant pressures exceed 410 bar. Programmatic goals that generally enforce weight minimization and associated performance requirements can result in thin walls ($<1\text{ mm}$) that must withstand high heat flux. The combination of harsh chamber conditions and thin hot walls results in high thermal gradients often exceeding 230°C through the wall, inducing high thermal stresses. In addition to demanding high performing tensile and fatigue properties, fracture toughness is essential due to potential impacts from domestic or foreign object debris (DOD or FOD). Depending on the environment corrosion resistance and wear resistance may also be required. Other environmental factors such as radiation, atomic oxygen, ultraviolet, or plasma may also place additional requirements on the properties required for a material. The operating environment thus drives the desired properties for an alloy including mechanical, physical and thermophysical. These properties are derived from the interconnection between the process-microstructure-properties ultimately leading to end-use performance.

Various traditional manufacturing processes and techniques for aerospace components are well-matured and the alloys produced from these processes well-characterized to produce flight components. These processes can include forgings, castings, machining, welding, brazing, inspections, heat treatment, and other assembly operations to fabricate the final component and system. The manufacturability and sequence of operations (including supply chain and processing economics) are necessary considerations for component and system designs but can lead to long lead times and cost increases. Additionally, propulsion components are often produced in low volumes (<100 units) and specialty process development can be costly if not fully amortized. While design and integration of components and system is arduous, the manufacturing stage is when most of the program problems arise. There are opportunities to improve or replace the existing manufacturing techniques to reduce costs and eliminate non-conformances. In addition to improving or replacing the manufacturing processes, there are opportunities for new alloys to enable higher performance.

Additive Manufacturing (AM) has matured rapidly for use in propulsion systems with many components in both flight and in developmental applications. AM has demonstrated schedule savings of 2–10x

over traditional methods and allows for regular and early developmental manufacturing and testing to iterate designs. Cost reduction has been continuously demonstrated using AM for complex components on the order of 50% or greater. To achieve these gains, AM must be applied intentionally and methodically to obtain potential technical and economic advantages with strong consideration of the alloy being used. While AM has shown advantages for cost and schedule reductions, it also offers new opportunities to alloy for higher performance alloys.

AM maturation started with a limited number of commonly available alloys – Ti6Al4V, AlSi10Mg, Inconel 625, Inconel 718, CoCr, and 316 L stainless steel for example [1,3]. This led designers to use what was available, but not always what provided the optimal design solution. Propulsion applications tend to be more risk-sensitive, so a design may lean towards the selection of common, accessible, and well-matured AM alloys over a new an AM alloy that needs to be developed, characterized, and matured [4]. As many AM processes have become standardized and more widely accepted, the adoption of new alloys for AM may readily occur with a greatly reduced developmental cycle per material. NASA specifically identified this need for various propulsion applications as well as the gap to develop and mature new alloys using AM processes. A specific goal in new alloy development was not only to increase the end-use alloy performance, but also ensure robust printing to eliminate issues that can arise during traditional manufacturing. Having the choice of new alloys that are intentionally enabled by AM could provide many benefits: expanded design options, improved product performance, and reduced post-processing costs. NASA has advanced AM alloys to meet end-use environments under alloy families such as copper, Fe-Ni, high temperature superalloys (i.e., ODS), and refractories. Each of these alloys has different target use applications and developed per requirements described previously. Alloys discussed in this paper include GRCop-42 (Cu-4 at.% Cr-2 at.% Nb) and GRCop-84 (Cu-8 at.% Cr-4 at.% Nb), NASA HR-1 (Fe-Ni-Cr), JBK-75 (Fe-Ni-Cr), GRX-810 (NiCoCr), C-103 (Nb-10 wt%, Hf-1wt%, Ti), Tungsten (W), and Molybdenum. The use temperature and purpose of these custom alloys is shown in Table 1. The unique category of oxide dispersion strengthened (ODS) nickels use a nanoscale oxide such as yttria (Y_2O_3), zirconia (ZrO_2), or thoria (ThO_2) for strength and creep improvements.

Several of these alloys have roots using traditional techniques but were not advanced due to challenges with production in the wrought form or economic reasons. In fact, alloys such as NASA HR-1 were developed using wrought and traditional processes then shelved for 15 years. AM has brought about rapid development with a reduced supply chain and build process schedule. This has revived interest in previously difficult-to-process alloys or new alloys only enabled by AM. The alloys described in this paper fill several gaps for materials needed in liquid rocket engine environments including hydrogen resistance, high pressure environments, extreme temperatures, creep resistance, and a combination thereof. This paper describes the importance of each of these AM alloys for propulsion, the development work completed on these including the formulation, AM build processes, characterization,

Table 1

Specialty AM alloys developed with different purposes for propulsion components.

Max. Use Temp. (°C)	Alloy Family	Purpose	Novel AM Alloys	Propulsion Use
200 750	Aluminum Copper	Lightweighting	–	Various
		High conductivity; strength at temperature	GRCop-42, GRCop-84	Combustion Chambers
800	Iron–Nickel	High strength and hydrogen resistance	NASA HR-1	Nozzles, Powerheads
900	Nickel	High strength-to-weight	–	Injectors, Turbines
1100	ODS Nickel	High strength at elevated temp; reduced creep	GRX-810, Alloy 718-ODS	Injectors, Turbines
1850	Refractory	Extreme temperature	C-103, C-103-CDS, Mo, W	Uncooled Chambers

heat treatment optimization, microstructure characterization, mechanical and thermophysical testing, and hot-fire testing. Proper maturation of the alloys requires a thorough understanding of the entire AM life cycle from component conceptual design through end-use service life to successfully implement.

2. AM processes and development

2.1. AM processing life cycle

The AM life cycle is inclusive of various steps that include the design and analysis of the part and build, the AM build processes with inputs including feedstock and build parameters, post-processing, and finally verification and certification before the part is placed into service [3]. Post-processing may include operations such as powder removal, support removal, build plate removal, heat treatments (i.e., stress relief, hot isostatic pressing (HIP), solution, aging, etc.), cleaning, inspections, machining, polishing, and joining. Since the AM process is tightly integrated through all process steps, there are many opportunities where defects can manifest or improper order of operations that can reduce performance. The manufacturing process derived for AM is much more than just printing the part. The successful development of new AM alloys integrates all the above steps.

Various AM processes have been matured to produce the NASA AM alloys for specific component applications [5]. The AM processes are categorized into melting processes and solid-state processes. Each has unique advantages and challenges, and many are supplemental to one another. The most commonly used AM processes to produce components are categorized into powder bed fusion (PBF) and directed energy deposition (DED). The PBF process, specifically laser powder bed fusion (L-PBF) manufactures parts using a bed of powder and a laser as the energy source. The laser melts the powder in a defined scanning strategy to create features within a discrete layer. The build chamber is fully purged and a recoater arm provides a new layer of powder to be melted in a layer-by-layer operation to build a complete component. L-PBF is most often used for fine feature components but is limited in overall build volume. GRCop-42, GRCop-84, GRX-810, C-103 all made use of L-PBF since these alloys are used in components that require small feature resolution such as combustion chambers and injectors.

Another AM process used to manufacture custom NASA alloys is DED, which has several variations based on feedstock and energy source (i.e., laser, electron beam, electrical arc). The most common DED method is laser powder directed energy deposition (LP-DED) providing medium resolution features, but exceptionally large build volumes. LP-DED uses a deposition head equipped with off-axis or coaxial nozzles, which blow powder into a melt pool formed by a laser. This deposition

head is attached to a gantry or robotic motion control and defined toolpath from the part CAD geometry. A local purge or fully inert build chamber is used to reduce oxygen and a trunnion table is typical of the motion control system allowing for multiple axis orientations for part deposition. The hydrogen-resistant NASA HR-1 and JBK-75 alloys were targeted for use with the LP-DED allowing for large scale integral channel wall rocket nozzles to be built. GRCop-42 and C-103 have also been built using the LP-DED process and plans are in place for GRX-810 LP-DED development.

AM build process selection is critical for parts to be produced successfully and for fully realizing economic benefits offered by AM. This was previously discussed in a detailed paper [3]. Attributes that can discriminate between the processes include overall part size, part complexity, feature resolution, process economics and availability, industrial maturity, post-processing, and metallurgical characteristics and properties. A typical input prior to process selection is the type of alloy. Each AM process has unique attributes and not all the novel alloys can be built using all the AM processes. Feedstock is an important discriminator as well. The alloys defined in this paper are readily available as a powder feedstock and are the most economical source for AM processes. GRCop-42 and GRCop-84 require gas atomization using argon to form the chromium-niobium in suspension for the dispersion strengthening [6]. NASA HR-1 and JBK-75 are produced using rotary atomization but can be produced using gas atomization [7]. C-103 and GRX-810 also use gas atomization. GRX-810, ODS, and carbide dispersion strengthened (CDS) family of alloys all require a coating process for the powder following atomization [8].

2.2. ICME modeling for novel alloys

Integrated Computational Materials Engineering (ICME) is a transformative discipline that enables rapid materials development through computational methods that integrate materials information with processing and performance [9]. Infusion of ICME into AM workflows provides numerous benefits such as rapid maturation of AM processed alloys from the initial formulation through development to production of flight-certified parts [10]. ICME approaches are experiencing broad adoption, extending beyond their traditional role as academic tools, primarily due to the reduction in the material maturation cycle. NASA is using such approaches to develop new alloys with optimal 3D printing characteristics including printability of new refractory alloys and enhanced mechanical performance of oxide dispersion strengthened nickel-based alloys. Two examples on the usage of ICME at NASA centers for the development of such materials is described here.

A first example of ICME implementation at NASA is the circumvention of difficulty and expense associated with conventional refractory metal manufacturing methods. Under conventional manufacturing methodologies, refractory metal and alloy bar, plate, tube, and sheet are fabricated through various forming and joining cycles leading to difficulties with machining a hard material, difficulty in producing defect-free joints, and high expense and material waste of high-value stocks. Additive manufacturing can mitigate much of the waste and expense but requires refractory metal and alloy feedstocks that are printable (resistant to formation of build defects). There is opportunity to reexamine the refractory metal alloy space using computational approaches combined with limited empirical validation to develop new printable alloys in the W, Nb, Mo, and Ta families.

Several metallurgical issues arise during printing of such materials: 1) solidification cracks occur during terminal stages of alloy solidification, 2) large grain formation due to epitaxial growth and thermally activated grain growth, and 3) a shift in ductile-to-brittle behavior to temperatures at or above the build temperature resulting in cracks as the grain size increases. The approach to mitigate these issues is through inoculation of powder feedstocks with high melting point intermetallic particles (examples include ZrC, TaC, HfC), which are optimized in size and distribution to pin grain boundaries thereby preventing grain

growth and associated embrittlement. Addition of these particles alters the solidification behavior and can unfortunately promote solidification cracking during the build. ICME tools (including CALPHAD and custom Python routines for solidification crack modeling and particle coarsening) are used to find regions of optimal powder addition where grain growth and solidification cracking are both minimized. Fig. 1 shows an example of hundreds of solidification cracking and particle coarsening simulations of the W-Zr-C ternary system, mapping out regions of cracking susceptibility. Darker contours suggest compositions where a new alloy would be most crack-resistant and lighter contours suggest compositions expected to be most crack susceptible. To map this space empirically would require hundreds of powders to be formulated and printed which is unequivocally cost prohibitive. Yet with ICME, the composition space can be mapped on a workstation in less than 24 h, and then validate computed findings empirically with a few select data points to guide production of future W and W-alloy powders using the inoculant addition approach.

A second example involves promising results from NiCoCr ODS alloy production using L-PBF at the NASA [8]. CALPHAD modeling was employed to produce a new ODS composition utilizing the equiatomic NiCoCr system as the foundational base chemistry. From these simulations a few notable findings were made. It was evident that Mo additions typically stabilized unwanted phases (e.g., σ , μ) and the ratio of Ti to Nb was critical for the stabilization of MC carbides especially at 1093 °C. Previous ODS alloys developed for AM indicated that grain boundary oxidation played a significant role in ultimate tensile strength and ductility variations. In turn, MC carbides were targeted to improve grain boundary strengthening and oxidation resistance [11]. The solid solution strengthening was targeted for improvement from existing Ni-based alloys while maintaining phase stability up to and at the target test temperature of 1093 °C. The freezing range was targeted to remain under 100 °C. Certain elements had unexpectedly large impacts on the freezing range and were assumed as unwanted additions for an alloy designed for printability. Unwanted phases, namely σ and μ , were effectively suppressed as low as 810 °C, hence the alloy was named GRX-810. The simulations suggested this new composition had the best balance between printability, strength, oxidation resistance, and phase/microstructure stability. Fig. 2 reveals the amount of each phase in the temperature range 800–1500 °C, as predicted by the thermodynamic model for GRX-810.

Both examples above provide a snapshot of thousands of virtual experiments that were enabled by ICME approaches. There is no need to create hundreds of new powder lots, fabricate thousands of samples, and then perform extensive material evaluations. Instead, commercial off-the-shelf and custom codes may be used to rapidly screen large

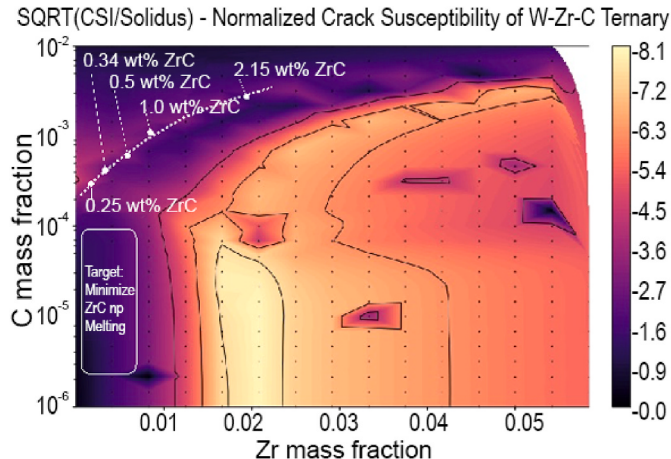


Fig. 1. Calculated solidification cracking susceptibility of the W-Zr-C ternary system. Dark contours represent regions of lowest cracking susceptibility.

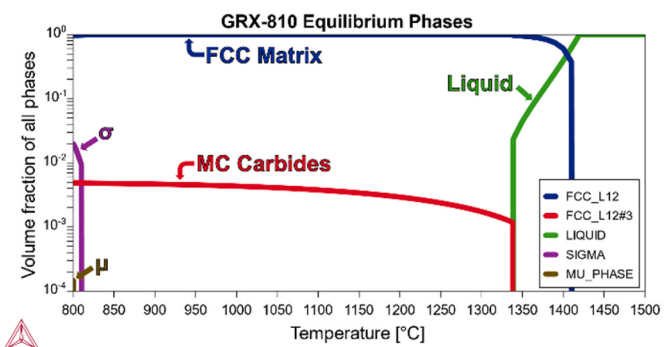


Fig. 2. Predicted phase stability of GRX-810 between 800–1500 °C. No detrimental phase formation is predicted above 810 °C.

composition spaces with a desired performance metric and optimize chemistry. Such techniques are being slowly adopted for propulsion applications. There is still tremendous opportunity available to infuse ICME into development cycles for next generation space propulsion alloys.

3. Maturation of alloys for propulsion

3.1. Alloy selection for propulsion components

Each component in a liquid rocket engine system must complete a methodical trade to determine the appropriate alloy requirements based on the environment, system loads, and life requirements. Combustion chambers operate at high heat fluxes from the combustion process and are most often actively cooled using the propellants (generally fuel) to maintain reasonable wall temperatures and avoid melting [12]. Copper-alloys are often used due to the high conductivity and strength at wall temperatures that can exceed 750 °C [13]. Low cycle fatigue (LCF) is often a key consideration as chambers must survive multiple starts and sustained duty cycles for reusability. Due to the environment from the propellants, oxidation can lead to blanching, and hydrogen can cause hydrogen environment embrittlement [14]. NASA has matured GRCop-42 and GRCop-84 to meet these requirements. The Glenn Research Center Copper- (GRCop-) alloys were developed as a high strength and high conductivity alternative to other commonly used copper-alloys such as C-18150 (Cu-1.5 wt% Cr-0.2 wt% Zr), NARloy-Z (Cu-3 wt% Ag-0.5 wt% Zr), Glidcop-15 (Cu-0.15 wt% Al₂O₃), and C-18200 (Cu-1.2 wt% Cr).

A general comparison of the copper-alloys is shown in Fig. 3 comparing conductivity with yield strength at elevated temperature (600 °C). A single plot is often difficult to capture the entire material trade since only two of the criteria are shown and can also change at elevated temperatures or different conditions. For instance, pure copper is limited to approximately 200 °C before it reaches a significant reduction in strength. Other copper alloys such as C-18150 and C-18200 are generally limited to nominal operating temperatures of around 540 °C due to reduced strength or changes in thermal properties due to the sustained temperatures.

Another key component in a liquid rocket engine is the exhaust nozzle, which is typically regeneratively-cooled (regen) due to the high heat flux. The joint between the chamber and nozzle is appropriately selected to balance the heat flux with minimizing overall system weight. While the chamber uses copper-alloys for high conductivity, the regen nozzle is made from a higher strength-to-weight alloy, typically a stainless steel or superalloy. The NASA HR-1 was specifically developed for regen nozzle applications using hydrogen as a propellant, allowing for hydrogen resistance which otherwise causes hydrogen environment embrittlement (HEE) issues. The NASA HR-1 variant for AM applications was specifically formulated for high ultimate strength, yield strength,

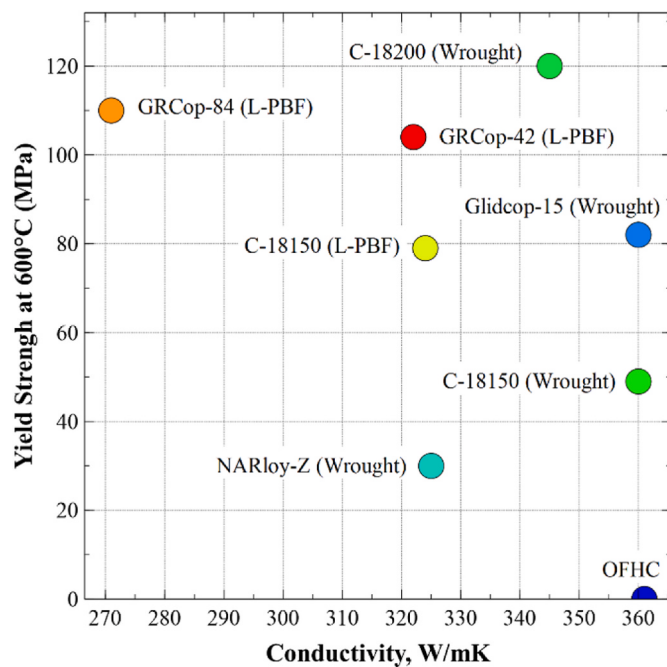


Fig. 3. Comparison plot of copper-alloy selection based on conductivity and yield strength at 600°C. Data compiled from Refs. [15–17].

and elongation in this environment and superior weldability, which translates into good printability. LCF is also a strong consideration in the nozzle design since it is tested and flown for multiple starts and missions. The conductivity was also improved in the LP-DED version of the alloy compared to the wrought version to aid with the design for nozzles.

A comparison plot is shown in Fig. 4 for various superalloys, stainless steel alloys and NASA HR-1 with the hydrogen embrittlement index (HEI) along with the ultimate strength at elevated temperature. While almost no metals are fully resistant to hydrogen, HEI values below about 20% are not as susceptible to embrittlement. The NASA HR-1 shows a

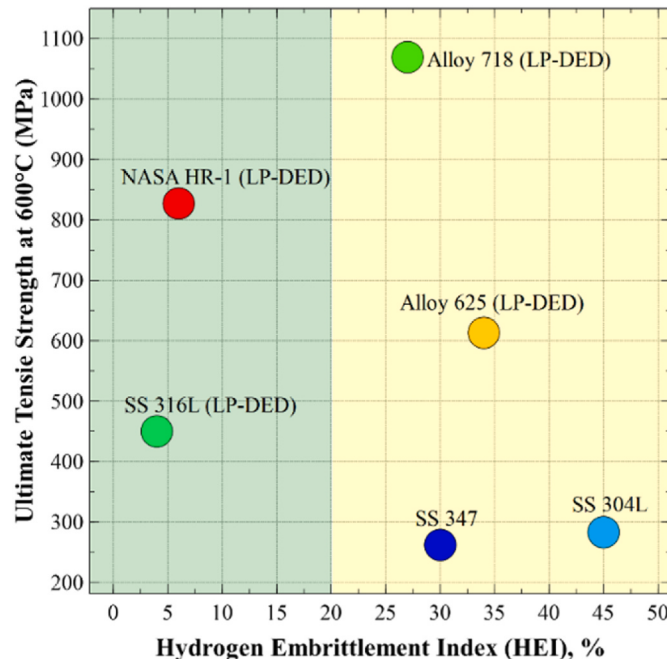


Fig. 4. Comparison plot of NASA HR-1, superalloys, and stainless alloys comparing the hydrogen embrittlement index (higher HEI = more susceptible) to ultimate strength at 600 °C.

very low HEI along with a high ultimate tensile strength (UTS) at 600 °C. This is a typical operating temperature for the NASA HR-1 alloy for regen nozzles, but nozzle operating temperatures can exceed this temperature based on the environment and engine requirements. Other alloys such as 316 L can meet the HEI requirement, but with a significant reduction in strength. Superalloys such as Alloy 625 (Inconel 625) and Alloy 718 (Inconel 718) can be used in this environment but will require a significant reduction in material properties and frequent inspections to account for the HEE. NASA HR-1 offers an excellent balance of the high strength, HEE resistance, LCF life, thermal conductivity, and ductility to meet the channel-cooled nozzle requirements for engines using hydrogen or other propellants (i.e., methane, liquid natural gas).

Propulsion components such as rocket injectors, nozzles, turbine blades, combustors, and other hot section components operate at elevated temperatures for sustained durations and multiple engine starts. Typically Ni-based superalloys are used in these environments but are generally limited to 900 °C or less in most cases for sustained operation. While γ' precipitate strengthened Ni-alloys can sustain some minimal mechanical properties at temperatures up to 1200 °C, this is not a realistic design temperature for this type of material. This can limit the performance of these components and the overall system may not be optimized due to temperature limits in a turbine or injector faceplate. Other challenges with current components include creep rupture, which is a necessary design consideration for sustained durations and high duty cycles such as those for aircraft engines.

GRX-810 (Glenn Research Center eXtreme) alloy was developed and is being further matured to allow an increase in operating temperatures for these various components. The alloy is Ni-Co-Cr-based and incorporates ODS coating of the powder to allow the high performance at elevated temperature. Traditionally manufactured ODS alloys were plagued with high expenses due to the manufacturing process [18], but AM is enabling more economical high performance ODS alloys, like GRX-810, to be produced. It is also enabling for high-complexity ODS alloy components such as injectors.

While operating temperatures and creep are a couple of considerations, the mechanical properties such as ultimate and yield as well as physical properties such as density need to be considered for optimal designs. The GRX-810 alloy compared to other superalloys and ODS superalloys is shown in Fig. 5. For reference, AM Ni-Co-Cr using L-PBF is also shown on the same graph but is without the yttria addition present in GRX-810. The strength of the GRX-810 with the ODS nearly doubles the strength at temperature. An additional advantage of ODS alloys includes improved oxidation properties at elevated temperatures by promoting and stabilizing Alumina or Chromia oxide scale formation [19]. The creep rupture life of GRX-810 increases orders of magnitude over more traditional Ni-based superalloys such as Alloy 625 and Alloy 718 at 1093 °C based on testing at NASA Glenn Research Center [20].

Refractory metals such as Niobium (Nb), Molybdenum (Mo), Tantalum (Ta), Rhenium (Re), and Tungsten (W) and their alloys are used for extreme high temperature environment service. Refractory metals are desirable due to a high melt temperature (T_m) and the ability to retain strength and hardness at elevated temperatures, but with the exception of Nb, they have higher densities than Ni-base superalloys [21]. Examples of applications include in-space radiatively cooled thrusters, reaction control system (RCS) thrusters, nuclear thermal propulsion (NTP) fuel and structure, hypergolic and green propulsion chambers, nuclear power system in-core heat pipes and heat exchangers, electric propulsion, and plasma facing components in fusion reactors. Refractory metals and alloys extend the operating temperature to between 1100 and 2500 °C, depending on the selected material, as shown in the red bullets in Fig. 6. Selection of a specific metal or alloy is highly dependent on expected operating conditions including temperature, environment (i.e., oxidizing, reducing, inert, vacuum), stresses, neutron fluence, etc.

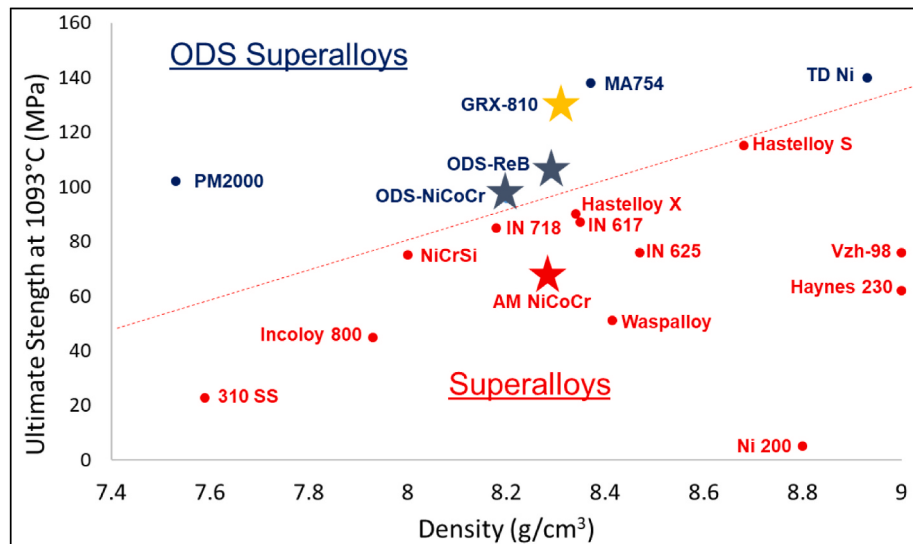


Fig. 5. Comparison of ultimate tensile strength at elevated temperature (1093 °C) with density for GRX-810 and other ODS alloys as well as Ni-based superalloys.

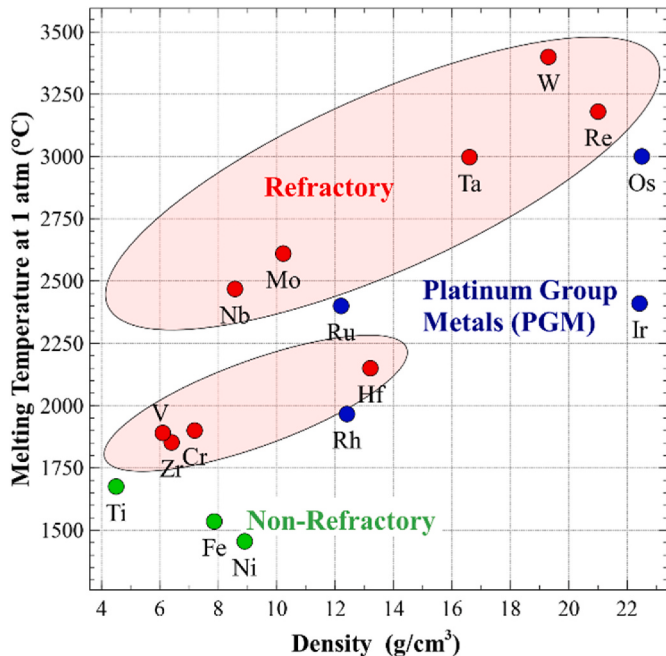


Fig. 6. Refractory elemental density compared to melting point at 1 atm.

4. High conductivity GRCop-42 and GRCop-84

The GRCop alloys are dispersion strengthened through Cr_2Nb precipitates created during the powder atomization and refined during L-PBF processing [22]. The GRCop alloys were specifically formulated for high strength at temperature, HEE resistance, high conductivity, and long low-cycle fatigue (LCF) lives. The chemical composition for GRCop-42 and GRCop-84 is shown in Table 2. The GRCop alloys also have improved oxidation and blanching resistance compared to most low-alloy Cu-based alloys [23,24]. GRCop alloys allow hot wall temperatures of ≥ 700 °C depending upon the strength, creep, and LCF requirements.

In 2014, NASA started development of the L-PBF process for GRCop-84 under the Low-Cost Upper Stage Program (LCSUP) and successfully built and hot-fire tested various chambers. Material and property characterizations were also performed [25]. While the GRCop-84 had high

Table 2
Chemistry of GRCop-42 and GRCop-84.

Element	GRCop-42 wt %	GRCop-84 wt %
Cu	Balance	Balance
Cr	3.1–3.4	6.2–6.8
Nb	2.7–3.0	5.4–6.0
Fe	Target < 50 ppm	Target < 50 ppm
O	Target < 250 ppm	Target < 250 ppm
Al	Target < 100 ppm	Target < 100 ppm
Si	Target < 100 ppm	Target < 100 ppm
Cr:Nb Ratio, wt. %	1.13–1.18	1.13–1.18

strength and good LCF properties, there was a desire to improve the thermal conductivity. NASA started L-PBF development of GRCop-42 in 2018 to mature the alloy through development of material properties, component demonstrations, and hot-fire testing. A critical task in developing these alloys were the establishment of the powder supply chain and commercial print services to permit accessibility of the GRCop alloys for commercial space use. As of 2023, more than eight international vendors are actively producing the GRCop powder and more than 12 commercial print services providing this as a standard material option.

An extensive effort was established to develop properties related to the GRCop alloys and to make these accessible to industry. Due to the dispersion strengthening, the GRCop alloys do not require heat treatment. Only a HIP is required to achieve full density. The typical tensile strengths as a function of temperature for L-PBF GRCop-42 and GRCop-84 is shown in Fig. 7. Advantages of GRCop alloys are high conductivity, good strength at elevated temperatures, and stability during operation [26]. The GRCop-84 has demonstrated higher strength at various temperatures due to the higher content of Cr_2Nb and slightly improved low cycle fatigue properties. The advantage of the GRCop-42 alloy is a 15–20% higher thermal conductivity as shown in Fig. 8.

NASA has utilized GRCop alloys in the manufacturing and testing of over 60+ combustion device components. The commercial space industry is also making use of GRCop-42 in development and flight applications. These include channel-cooled chambers, injectors, and ignition systems using L-PBF. Additional development work has been completed using the LP-DED process, but no components have been tested using this process as of this publication. NASA has successfully hot-fire validated chambers at over 1200 starts and greater than 45,000 s of cumulative duration as of this publication. One GRCop-42 L-PBF chamber was successfully tested with over 10,000 s and 293 starts, and a

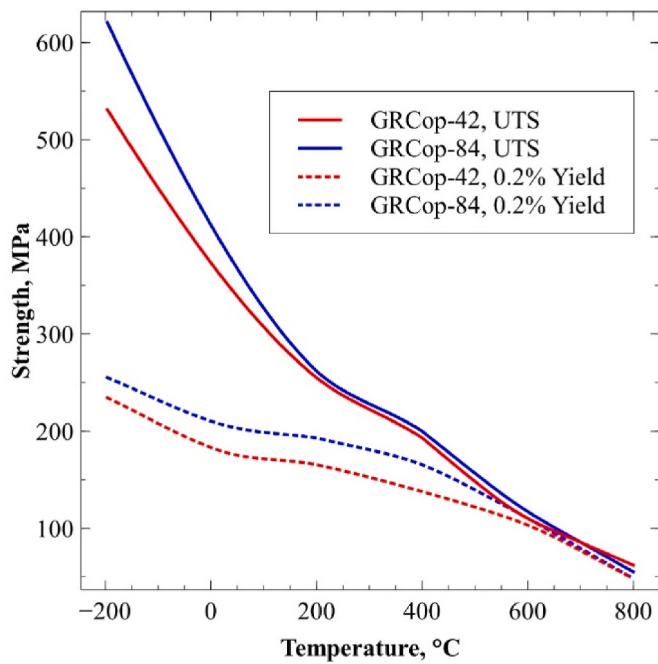


Fig. 7. Typical average ultimate tensile and yield strength vs. temperature for L-PBF GRCop-42 and GRCop-84 alloys.

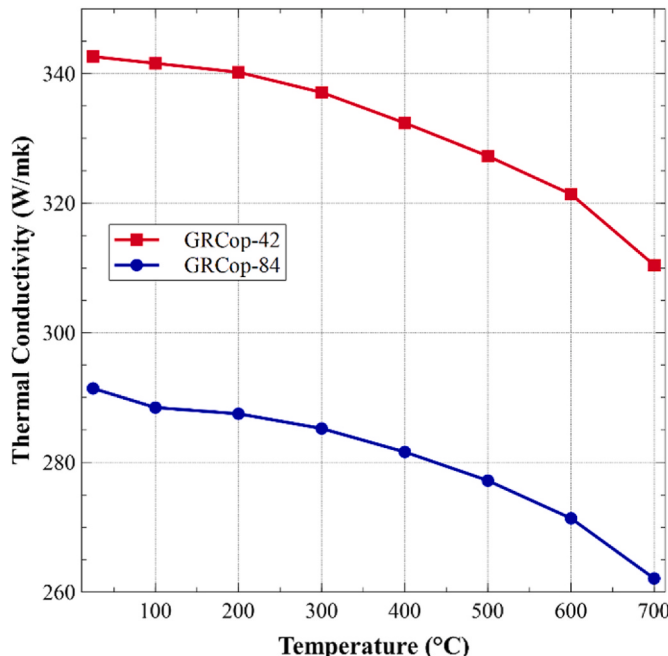


Fig. 8. Average conductivity vs. temperature for L-PBF GRCop-42 and GRCop-84.

second chamber achieved over 7400 s and over 168 starts. GRCop alloys have also enabled the development and long-duration testing of new propulsion concepts such as Rotating Detonation Rocket Engines (RDRE) [27]. These statistics demonstrate the robustness and versatility of the GRCop alloys. No damage to the chambers from blanching or cracks were observed. NASA has completed testing in Liquid Oxygen/Hydrogen (LOX/H₂), LOX/Kerosene (LOX/RP-1), and LOX/Methane (LOX/CH₄) using various GRCop-42 and GRCop-84 chambers. Examples of hot-fire testing and development chamber units are shown in Fig. 9.

Furthermore, the potential for rocket propulsion applications using

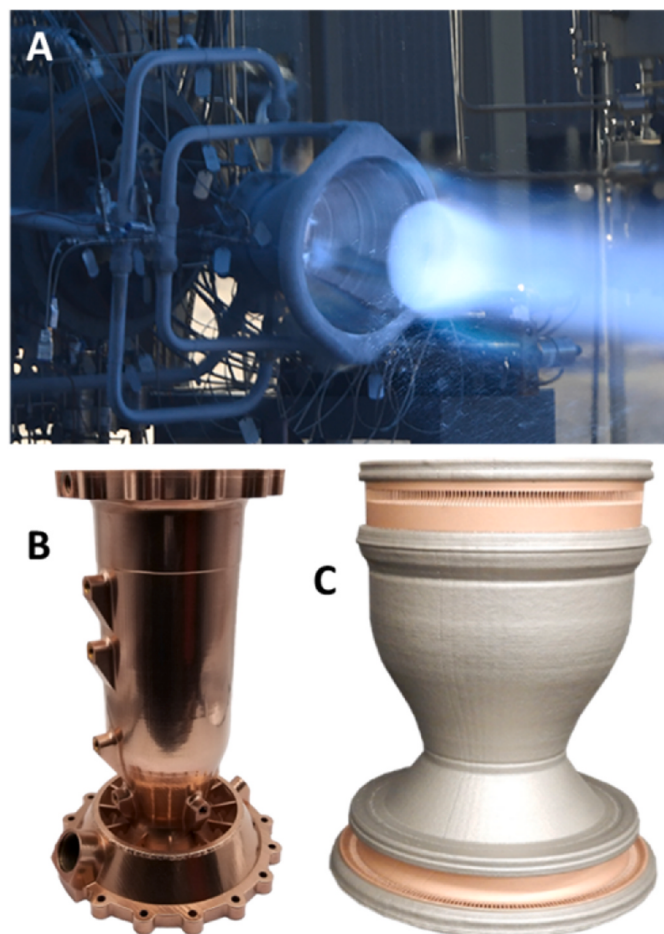


Fig. 9. Development and hot-fire testing of GRCop-alloy chambers. A) Hot-fire testing of a 31 kN LOX/CH₄ lander GRCop-42 chamber for 51 cycles, B) Polished GRCop-42 chamber, C) Bimetallic chamber using L-PBF GRCop-42 liner and NASA HR-1 LP-DED jacket.

GRCop alloys has been found to be extensive. L-PBF of GRCop alloys has been demonstrated for custom and complex designs to balance heat transfer and friction factors (pressure drop). Customization of surface roughness, waviness, and porosity in the L-PBF process allows engineers a broader trade space for liquid rocket engine design. High porosity allows production of transpiration features for active cooling of components such as an injector faceplate. Surface roughness reductions or increases allow for the customization of the desired engine heat load balanced with increasing or decreasing friction factors within the chamber channels. This impacts downstream component performance such as injector combustion efficiency by controlling coolant exit temperature and turbopump power requirements. Lastly, while oxygen compatibility of GRCop alloys has not been quantified, observations from hot-fire testing suggests high tolerance to oxygen rich combustion environments.

Additional development using GRCop alloys has been demonstrated using multiple alloys with various AM processes (bimetallic or multi-metallic). This has allowed for the high conductivity and high strength GRCop liner and a higher strength-to-weight alloy, such as Alloy 625 or NASA HR-1 to be used as a structural jacket. Additional development under NASA's Rapid Analysis and Manufacturing Propulsion Technology (RAMPT) project using axial bimetallic methods with GRCop-42 have enabled larger thrust chamber assemblies with multiple alloys and elimination of a bolted joint between the chamber and nozzle [28].

NASA has designed, produced, and tested GRCop alloy calorimetry chambers. These chambers have provided heat flux profiles for constant

pressure and rotating detonative combustion devices (i.e., RDRE) [29, 30]. GRCop alloys provided the properties to enable these high heat flux applications. The versatility of GRCop alloys is substantial, and an investment NASA will continue exploring along with commercial partners.

The powder production process and L-PBF process parameters have been fully commercialized and are in use across the propulsion industry. Development has also started using LP-DED to build parts with infrared and green wavelength lasers for monolithic and bimetallic components. An example of demonstrator chambers using GRCop-42 and GRCop-42/Alloy 625 green laser LP-DED manufacturing technology is shown in Fig. 10.

5. Hydrogen resistant NASA HR-1

NASA HR-1 is a high strength Fe–Ni based γ' -strengthened superalloy designed to resist high pressure hydrogen environment embrittlement (HEE), oxidation, and corrosion [2]. NASA HR-1 was originally derived from JBK-75 for increased strength and ductility in high-pressure hydrogen environments to meet the requirements of liquid rocket engine (LRE) applications. NASA HR-1 was developed to maximize yield strength, thermal conductivity, ductility, and LCF while minimizing HEE resistance. To achieve this, the chemical composition of NASA HR-1 increased γ' forming elements (Ti and Al), added W and Co, and adjusted the Fe and Ni content [31]. Wrought NASA HR-1 requires costly and tedious processing that was not economically feasible for LRE components. However, powder AM processes, such as LP-DED, have enabled NASA HR-1 to be a more affordable alloy for LRE applications. While adapting NASA HR-1 to the LP-DED process, it was discovered that the LP-DED process promotes Ti segregation and formation of detrimental η -phase more than the conventional wrought process [32, 33]. As a result, the composition of NASA HR-1 was modified to the final AM variant revision shown in Table 3. The changes made were expected

Table 3
Nominal chemical composition for AM NASA HR-1.

Element	NASA HR-1 Rev 3 wt% Range	NASA HR-1 Rev 3 wt% Target
Fe	BAL	41.2
Ni	33.7–34.3	34
Cr	14.3–14.9	14.6
Mo	1.6–2.0	1.8
V	0.28–0.32	0.3
W	1.4–1.8	1.6
Co	3.6–4.0	3.8
Ti	2.2–2.6	2.4
Al	0.23–0.27	0.25

to moderately decrease strength of the LP-DED alloy while improving the ductility, LCF life, and HEE resistance from the initial composition tested in LP-DED [34].

Significant development of heat treatments and material characterization for LP-DED NASA HR-1 began in 2019 to understand and optimize the microstructure of LP-DED NASA HR-1 [3]. Upon discovery of Ti segregation and η -phase problems, the subsequent powder composition adjustments also required further adjustments to heat treatments to mitigate η -phase as it can severely impact the HEE resistance of NASA HR-1 [4]. Changes to the stress relief, homogenization, and solution treatment times and temperatures helped to minimize Ti segregation due to the LP-DED process, and the aging cycle was changed from a 1-step to a 2-step age as this was observed to mitigate η -phase while minimizing the yield strength drop and improving ductility [5].

Once the heat treatments were determined, efforts focused on characterizing the mechanical and thermophysical properties of NASA HR-1. Tensile and low cycle fatigue have been tested across a range of temperatures and testing has been performed in pressurized gaseous Hydrogen (GH2) environments to assess the HEE resistance of LP-DED NASA HR-1 [35]. The ultimate tensile strength of various LP-DED alloys compared to NASA HR-1 is shown in Fig. 11. Using either the 1-step age for higher strength or the 2-step age for more ductility, NASA HR-1 performs between alloys 718 and 625. Compared to wrought NASA HR-1, LP-DED NASA HR-1 has lower strength but higher ductility showing one of many differences between wrought and AM materials [5]. Additionally, LCF testing has shown that LP-DED NASA HR-1 performs well across temperatures ranging from -196°C to 760°C (Fig. 12)

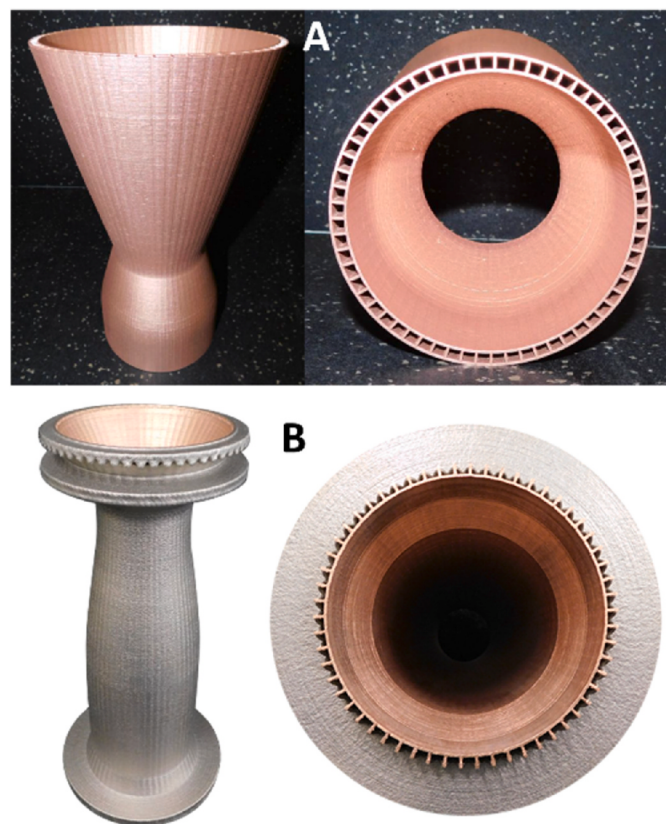


Fig. 10. Manufacturing demonstrator chambers using A) GRCop-42 and B) GRCop-42/Alloy 625 LP-DED green laser. [Courtesy: RPMI/TRUMPF/NASA].

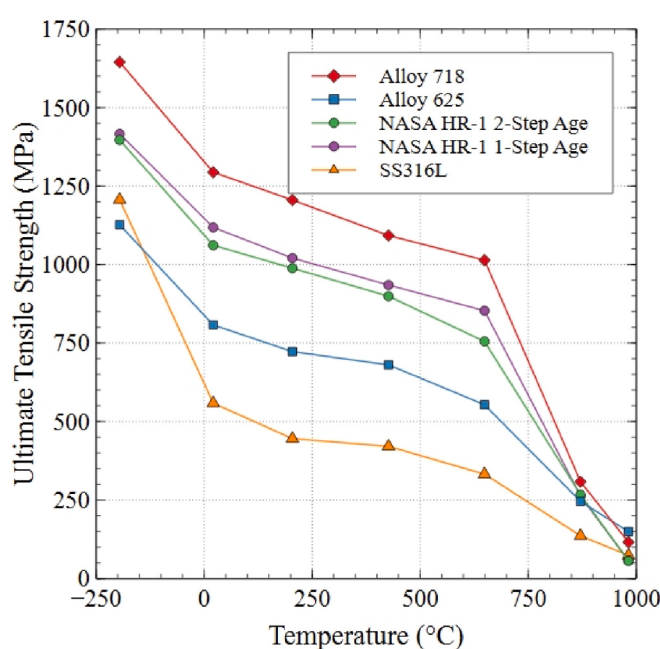


Fig. 11. Average ultimate tensile strength of LP-DED alloys versus temperature.

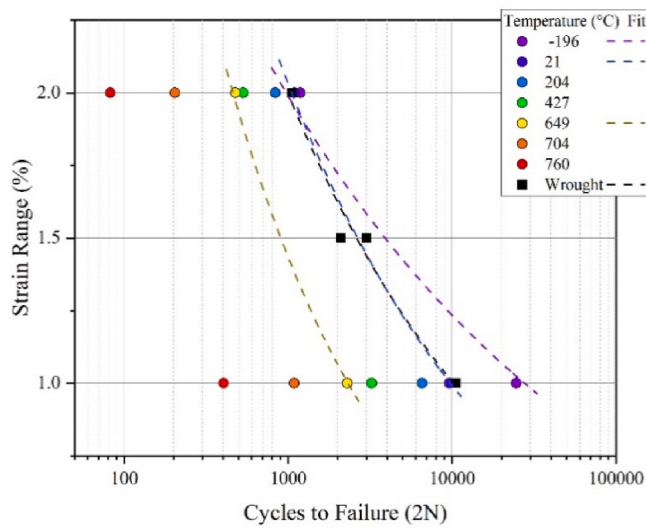


Fig. 12. Average LCF life of 2-Step aged LP-DED NASA HR-1 with changes in temperature compared to wrought values in GHe from [2,6].

and has equivalent or slightly lower LCF life at room temperature compared to wrought NASA HR-1 tested in gaseous Helium (GHe) [5,6]. A 1-step aging cycle was shown to increase strength with a slight detriment to low cycle fatigue life. These differences in mechanical properties can be attributed to compositional and microstructural differences between the wrought and LP-DED material. A study on thin-wall builds with reused powder has also been completed with LP-DED NASA HR-1 and indicated no debit to tensile or LCF properties after six reuses [36].

Thermal conductivity is another key property for LP-DED NASA HR-1, and test results are shown in Fig. 13 where NASA HR-1 is compared to other LP-DED superalloys. The conductivity for NASA HR-1 is very similar to Alloy 625 and Alloy 718 and showed an improvement over wrought NASA HR-1 [5].

NASA HR-1 alloy has been successfully demonstrated for various

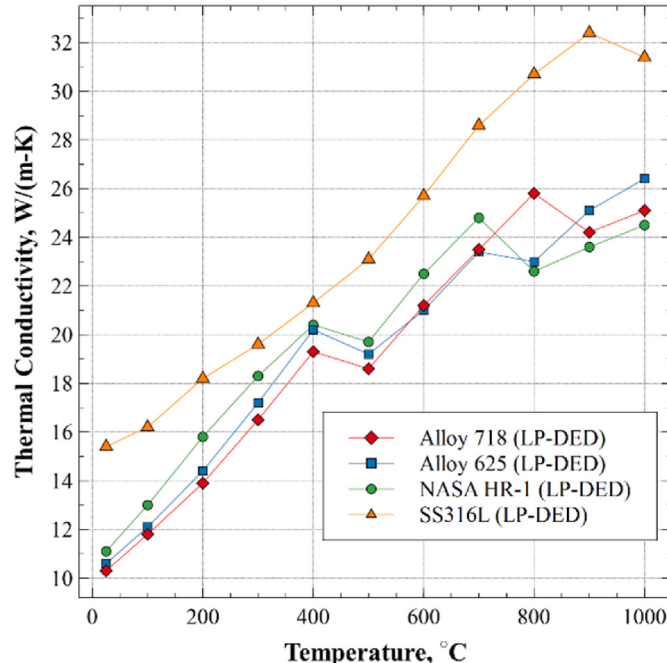


Fig. 13. Thermal conductivity of LP-DED NASA HR-1 and other LP-DED alloys vs temperature.

combustion device components targeting channel wall nozzles. The LP-DED process has shown robustness to produce large structures with integral coolant channels as well as thicker wall components for forging and casting replacements. Various parameters and corresponding laser melt pools can be varied to allow for different features. A lower power allows for thin walls to be deposited at 1-mm thickness for channel wall nozzles [37]. The higher power increases the deposition rates for thicker wall components that are often final machined and have limited internal features. The components demonstrated include powerhead half shells (i.e., for the RS-25 Engine's powerhead), manifolds for nozzles and chambers, transfer tubes, domes, and other pressure loaded components that are used in hydrogen environments. The LP-DED process was also used to build a manufacturing technology demonstrator (MTD) at 1.52 m diameter and 1.78 m height, approximately a 65% scale RS-25 channel wall nozzle (Fig. 14).

NASA has completed several test campaigns to demonstrate nozzles manufactured using the NASA HR-1 alloy with the LP-DED process. Testing of a 31 kN nozzle under NASA's Long-Life Additive Manufacturing Assembly (LLAMA) project demonstrated 40 starts and 568 s in a LOX/CH4 environment (Fig. 15A and B). The chamber pressure of this assembly was 52 bar, and the mixture ratio was approximately 3.2. Another test campaign using LOX/GH2 demonstrated high-duty cycle hot-fire testing of a NASA HR-1 LP-DED nozzle. Conditions were 8.9 kN thrust, and the nozzle achieved 207 starts and just under 6800 s (Fig. 15F). This demonstrated temperatures exceeding 760 °C on the nozzle hot wall with a chamber pressure over 76 bar and mixture ratios up to 7.5 using LOX/GH2 propellants. Additional NASA HR-1 LP-DED units were tested under this campaign with unique design features including a scalloped hot wall (tube-like) and spiral channels (Fig. 15E). All units performed as intended and met performance predictions. Two additional NASA HR-1 LP-DED channel wall nozzle units completed manufacturing and successfully tested using LOX/LH2 at the 156 kN thrust level (Fig. 15C and D). These units included a spiraled channel design and incorporated NASA HR-1 LP-DED manifolds. The deposition time for the nozzles were approximately 14 days and the manifolds were about 3 days each compared to 6+ months for conventionally



Fig. 14. 65% scale RS-25 integral channel LP-DEN nozzle using NASA HR-1 (1.52 m dia. X 1.78 m height).

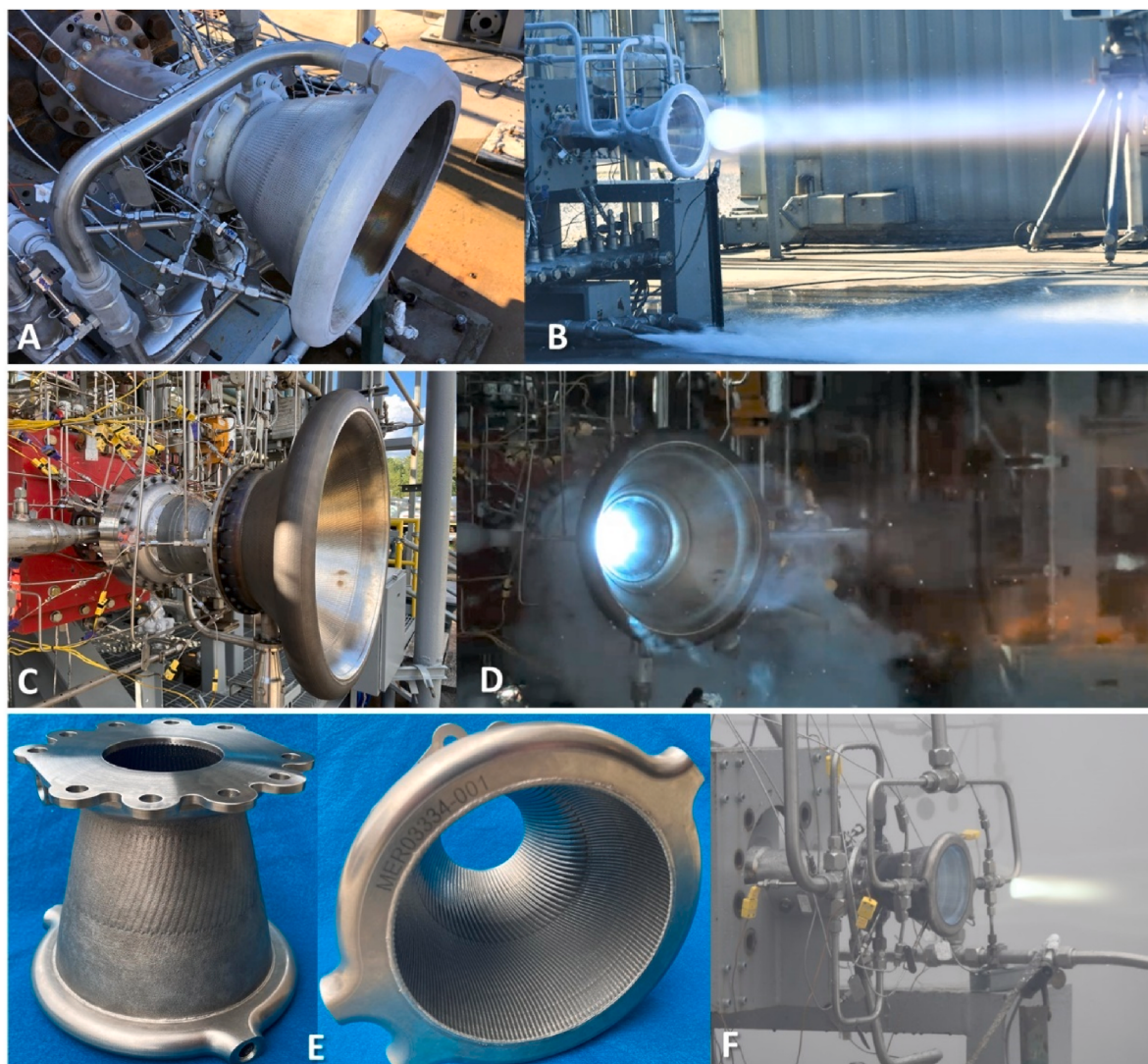


Fig. 15. NASA HR-1 nozzle test units. A, B) 31 kN integral channel LP-DED nozzle tested in LOX/methane and LOX-cooled, C,D) 156 kN thrust chamber assembly and testing E) Spiral tube-like hot wall LP-DED nozzle, F) Hot-fire in LOX/hydrogen testing of 8.9 kN nozzle that accumulated 207 starts and 6800 s.

manufactured nozzles. NASA has tested multiple integral channel wall nozzles (Fig. 15B) made with LP-DED NASA HR-1 and accumulated over 280 starts and 8914 s in hydrogen environments. A total of 313 starts and 10,140 s of hot-fire testing has been accumulated across eight NASA HR-1 alloy LP-DED nozzles as of 2022.

6. High temperature superalloy GRX-810

GRX-810 is a NiCoCr-based ODS alloy specifically developed for AM. The equiatomic NiCoCr system has been shown to be quite amenable to AM [38–40]. This has been attributed to the alloys narrow melting/freezing temperature range, the difference between the solidus and liquidus [41]. These studies have reported that the alloy maintains a solid solution in both the as-built and heat-treated conditions [40,41]. In addition, the AM-produced NiCoCr alloy provides exceptional ductility and strain hardening, comparable to its wrought counterparts. In order to further improve the high temperature properties of the NiCoCr alloy, a coating process for the AM powder feedstock was matured to produce oxide dispersion strengthened components as described by Smith et al. [41]. From this work, three different alloys were explored with the composition shown in Table 4. Notably, out of the three compositions, GRX-810 provided magnitudes of order better creep strength compared to the NiCoCr-ODS and NiCoCtReB-ODS [42].

Table 4
Compositions of ODS alloys explored and developed at NASA (wt.%).

Element	Alloy		
	NiCoCr-ODS	NiCoCtReB-ODS	GRX-810
Ni	BAL.	BAL.	BAL.
Co	32	32	33
Cr	30	30	29
Re	–	1.5	1.5
Al	–	–	0.3
Ti	–	–	0.25
Nb	–	–	0.75
W	–	–	3
C	–	–	0.05
B	–	0.003	–

To produce ODS GRX-810 components, pre-alloyed base powder with the above composition is coated with <1 wt% Y_2O_3 nanoparticles. Through L-PBF AM print parameter optimization, these nanoscale oxides are randomly and evenly dispersed throughout the microstructure as can be seen below in Fig. 16.

Scanning electron microscopy images of HIPed GRX-810 reveals a solid solution microstructure with Nb and Ti-rich MC carbides along

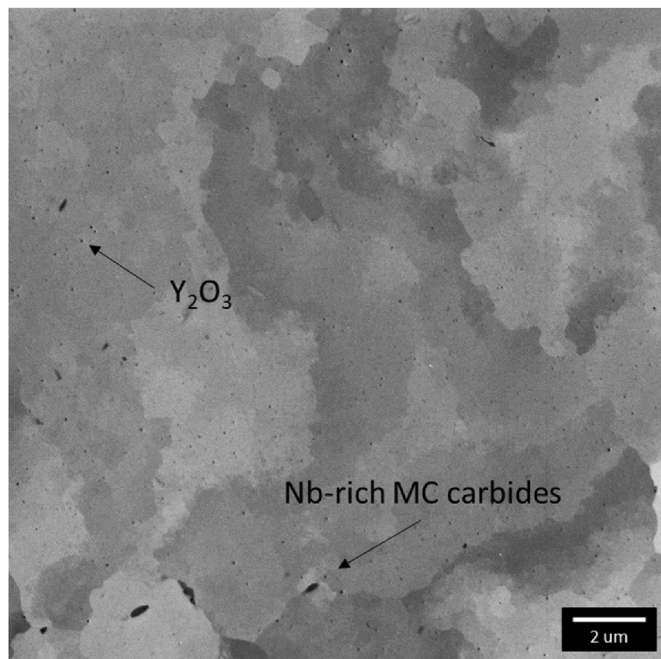


Fig. 16. A scanning electron micrograph of HIPed GRX-810 revealing a solid solution matrix with grain boundary Nb-rich MC carbides and dispersed nanoscale Y₂O₃ particles.

grain boundaries. Nanoscale Y₂O₃ particles can also be observed, though the resolution of this imaging technique cannot provide quantifiable characterization. Notably, no bulk oxide or slag formation was observed in these samples. From the micrograph in Fig. 16 it is apparent that the as-built grain structure is retained even after a high temperature/high stress HIP cycle. This provides evidence that the oxides are well distributed and can maintain and stabilize the microstructure at much higher temperatures as compared to non-ODS alloys. Though early in the alloys development phase, it presents promising mechanical results compared to the previous NiCoCr-ODS alloys as well as conventional superalloys. The tensile and yield strengths for HIPed GRX-810 were tested from cryogenic temperatures up to 1093 °C. Test results are shown below in Fig. 17 (full data in Appendix, Table A).

From Fig. 17, GRX-810 presents excellent tensile properties, specifically when present in extreme environments (cryogenic and high temperature). The ductility of the alloy remained above 30% at every temperature tested including cryogenic temperatures where it also exhibited high strengths. Fig. 18 compares the tensile strength of GRX-810 to wrought Alloy 718 and 625. Below 900 °C, tensile properties are higher for the precipitation strengthened superalloy 718 material. However, at temperatures above 900 °C, the 718 precipitates begin to over-age and eventually dissolve at the highest temperatures. In addition, grain growth becomes detrimental to non-ODS alloys impacting the strength at elevated temperatures. For GRX-810, this reduction in strength is much less pronounced due to the presence of the nano oxides throughout its microstructure which pin grain boundaries. Therefore, GRX-810 presents higher strength than what was possible with non-ODS conventional superalloys at temperatures above 900 °C. In Fig. 18 GRX-810 is compared to Alloys 625 and 718. These alloys are amenable to the AM process and used extensively for high temperature AM components. Therefore, it is important that GRX-810 can also be printed using AM techniques. In Fig. 19, images of complex geometries and components that have been built with ODS feedstock is shown. Successful hot-fire testing of multiple GRX-810 injectors and regeneratively-cooled nozzles was conducted at NASA MSFC using LOX/LH₂ and LOX/LCH₄ propellants at the 31 kN thrust level (Fig. 19C).

Fig. 19 presents evidence of the printability of the coated NiCoCr

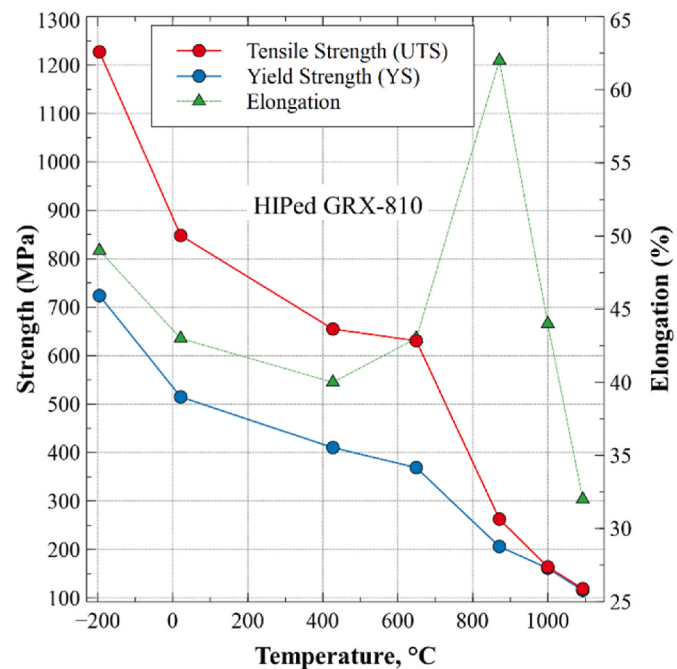


Fig. 17. The tensile properties of HIPed GRX-810 as a function of temperature.

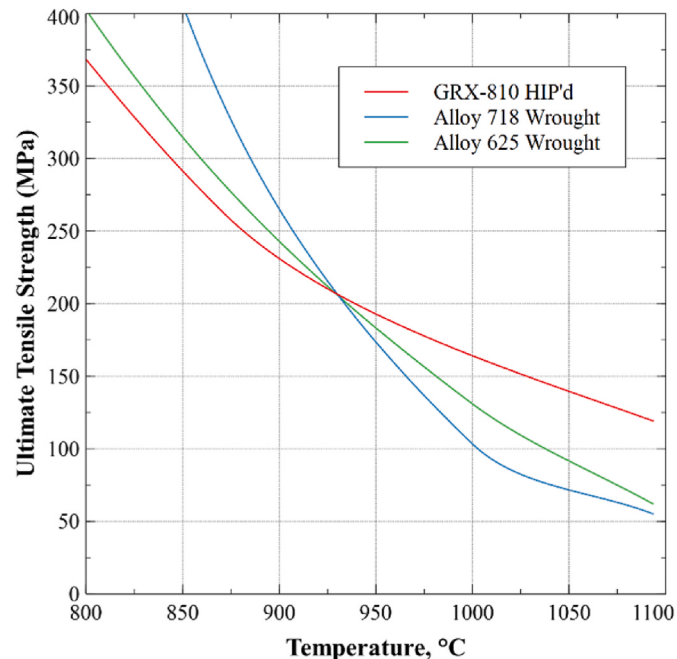


Fig. 18. Comparison of the elevated temperature tensile properties of GRX-810 compared to conventional wrought superalloys 718 and 625.

family of powders and the ability to additively manufacture components that may possess better properties than what is currently possible with conventional materials and manufacturing techniques. The technology to coat and build AM ODS components is not just possible in Ni-alloys but is speculated to improve the fabrication of difficult to print refractory alloys or improve the properties of currently printed Cu- and Ti-based alloys. GRX-810 represents a new class of AM materials that is rapidly maturing.

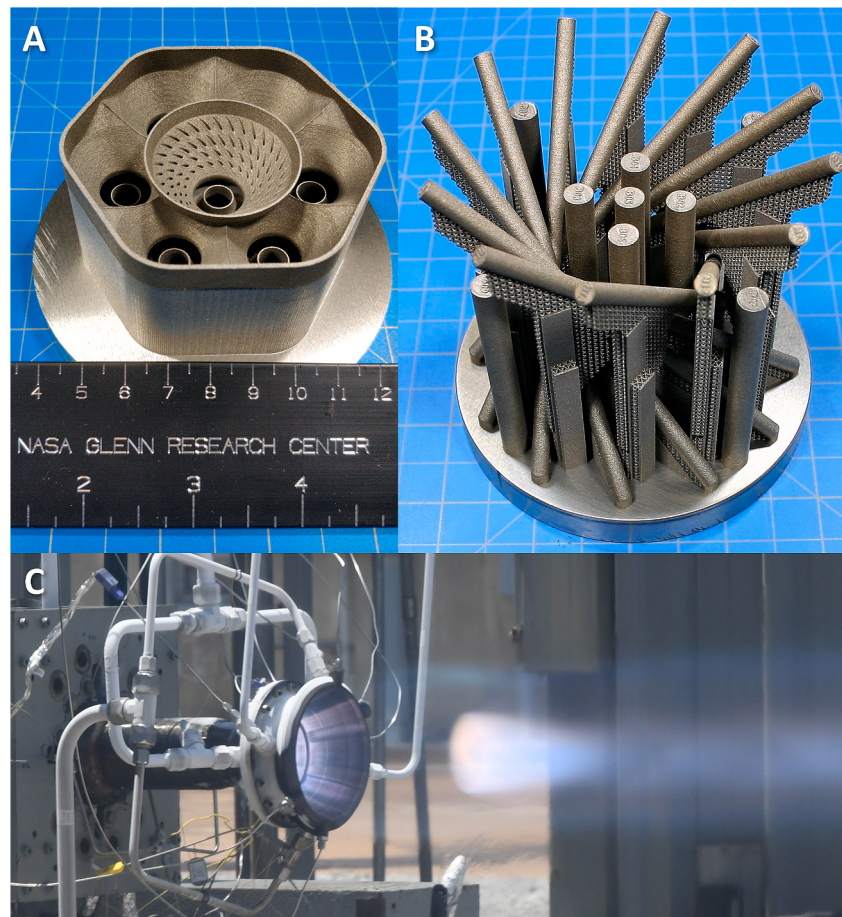


Fig. 19. a) An oxide dispersion strengthened 3D printed combustor dome and (b) complex lattice structures, (c) LOX/Methane hot-fire testing of a GRX-810 injector and nozzle.

7. Extreme temperature refractory alloys

Traditional refractory metal manufacturing is typically expensive due to the high material cost, specialized powder production methods, and unique machining and joining methods. Specific difficulties exist in forming parts due to high ductile-to-brittle transition temperatures, ultra-high temperature heat treatments, specialized oxidation coatings, and non-destructive evaluation (NDE) requirements also provide significant challenges in manufacturing refractory components [43]. Aerospace refractory metal parts tend to be thin-walled (i.e., converging-diverging nozzles) resulting in 95–98% of the stock being machined away. Thus, the cost of feedstock for a part is 5% for the actual part and 95% in machining waste. Machining and waste disposal add additional costs on top of the feedstock.

Other manufacturing methods are deposition-based such as vacuum plasma spray, electro-deposition, etc., and tend to be slow and expensive processes. They normally require mandrels that need to be removed post deposition and that limit part complexity. Due to the difficulty in traditional refractory metal manufacture, there are a limited number of vendors with the requisite equipment and experience [43].

AM refractory development is a rapidly growing field in AM and has been conducted primarily with EB-PBF, L-PBF, binder jet, EW-DED, and LP-DED AM. In most cases, these methods show a significant cost and schedule savings [4]. AM of C-103 is an example. Cost of an AM C-103 part has been found to be significantly less than the same part produced by conventional C-103 manufacturing, even when taking into account powder feedstock costs, print time, heat treatment, final machining, and waste disposal [44]. L-PBF and LP-DED AM C-103 is now available from several commercial AM suppliers to meet increasing demand. AM waste

from over-sized powder, support structures, and sacrificial geometric features to be machined away to meet surface finish requirements is typically only 5–10% of the printed part mass.

W, Mo, Ta, Re, and various alloys of these have also been produced with AM techniques but with a wide range of results [45]. Although printable, there is a markedly lower level of maturity due in large part to limitations in powder suppliers that can provide pre-alloyed powder that meets AM process specifications and a lack of high temperature mechanical testing that can meet relevant environmental conditions. Commercially available elemental AM grade powder options are expanded but currently limited to W, Mo, Ta, Re, and Nb; while available alloy powders include C-103 (Nb-10Hf-1Ti-0.7Zr), Ta3W, Ta5W, Ta13 W, FS85 (Nb-28Ta-10 W-1Zr), TZM (Mo-0.5Ti-0.08Zr-0.02C), W-25Re, and Mo-44Re (numerical values have units of wt.%). Custom refractory high entropy alloys (RHEA) are in development and are being optimized for AM leveraging CALPHAD.

AM refractory metal components suffer from decreased mechanical properties compared to traditional manufacturing methods not only due to AM induced micro-cracking but also grain growth at elevated operating temperatures [43]. Materials that are strengthened by fine grain AM microstructure can become ineffective at elevated temperatures as grain growth occurs. Refractory metals are known to experience this phenomenon. Carbide-dispersion strengthened (CDS) process is one of the options under development at NASA to not only address micro-cracking during the AM process but also to pin grain boundaries and retain mechanical properties at expected operating conditions. Nano powder dispersoids can be mixed with parent metal powder prior to the AM process similar to the ODS GRX-810 alloy or can be precipitated during heat treatment, such as HfO₂ in AM C-103 as shown in

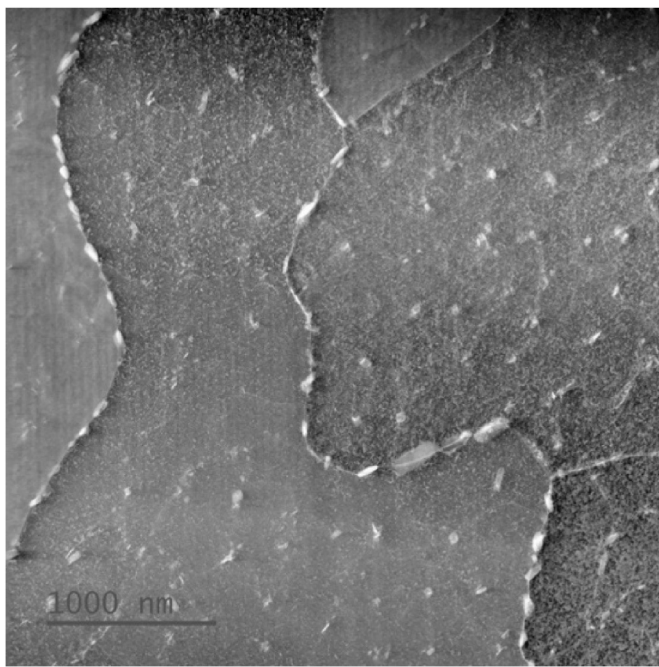


Fig. 20. Transmission electron micrograph (TEM) of L-PBF AM as-built C-103 HfO_2 precipitate distribution [43].

Fig. 20. Note on the figure that dispersoids are the brighter particles that are present along grain boundaries and interdendritic regions within the darker matrix phase.

Development of AM C-103 for NASA was completed using L-PBF along with vacuum stress relief at 1100 °C and a HIP cycle to optimize properties of the alloy [44]. The achieved density exceeded 99.98% of the theoretical density in as built and further increased following HIP. There was no substantial grain growth following stress relief. Mechanical property testing of the L-PBF demonstrated the ability to achieve properties comparable and in some cases higher than wrought. AM C103 met specification minimums as well [46]. A comparison of 25 °C and

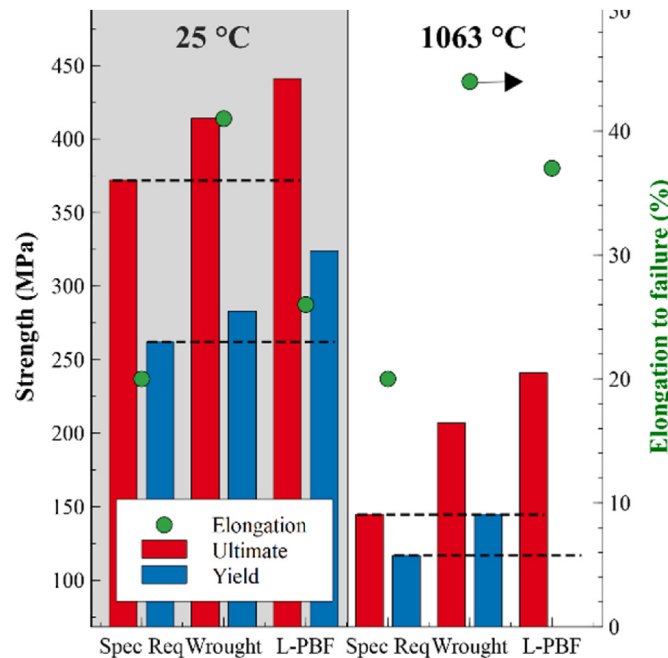


Fig. 21. Wrought vs. L-PBF C-103 ambient and elevated temperature mechanical property comparison [44].

1063 °C tensile properties are shown in **Fig. 21**. Additional process development with C-103 using LP-DED has also been successfully demonstrated.

Development of pure tungsten was demonstrated using L-PBF for complex thruster components and fine lattice structures as fine as 100 μm strut thickness [47]. L-PBF tungsten has also been demonstrated for a simulated 1 N thruster and inductively heated to 2300 °C as shown in **Fig. 22**.

8. Summary, outlook, and future work

Novel alloys are important to advance performance goals such as temperature and pressure capability, corrosion and wear resistance, and fatigue life in propulsion components. AM has demonstrated significant schedule and cost reduction to manufacture propulsion hardware and is being used to create complex designs as it both replaces and augments traditional manufacturing techniques. This paper emphasizes the importance of AM implementation that is deliberate and systematic to obtain the full potential of technical and economic advantages. With an in-depth understanding of various AM processes and their applicability with respect to feedstock materials, NASA has advanced many commonly available AM alloys. These AM alloys, including Copper-, Iron-, Nickel-, and Refractory-based alloys, have been inserted into various propulsion applications. Novel alloys being advanced using AM include GRCop-42, GRCop-84, NASA HR-1, GRX-810, C-103, C-103 CDS, Mo, and W for specific use in rocket engines for higher performance. However, there still exists a need to develop other metallic alloys that are only possible to produce with AM to further increase engine performance. They will enable higher operating temperatures, increased pressures, and longer life in challenging environments such as oxygen-rich staged combustion engines.

NASA has demonstrated various use applications of AM metal alloys matured and in development for rocket-propulsion components. This work covered the entire life cycle of AM starting from formulation, AM build processes, characterization, heat treat optimizations, microstructure characterization, mechanical and thermophysical testing, and finally ending with the engine level hot-fire testing. As of early 2023, NASA has accumulated over 100,000 s and 2300 starts on various AM hardware including injectors, chambers, nozzles, turbomachinery, and ignition systems with many of these using the novel alloys discussed in this paper.

Activities focused on AM optimized alloys and their process development for high performance applications will continue to be prevalent in the next 10 years, mainly because of the rapid technology advancement to be made in ICME. Success in these activities will not only benefit

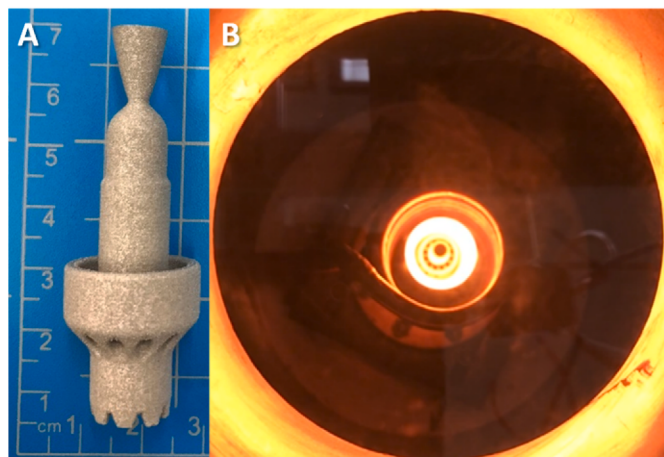


Fig. 22. A) L-PBF Tungsten 1 N green propulsion chamber, B) heated to 2300 °C.

NASA but the entire AM supply chain as well as the global space economy. AM has become one more tool in the manufacturing toolbox and is being accepted for fundamental rapid alloy development and production of components.

While there are still many lessons learned in the characterization of metal AM parts and alloys, the AM processes are becoming more widely adopted. In addition, the local aspect of AM, where organizations are now largely responsible for material integrity that is essential to their component production, cannot be ignored, particularly with new alloys. The immediate impact is a new emphasis on being integrated across disciplines and throughout the life cycle of AM components and assemblies. To successfully integrate these AM alloys requires discipline to define and follow a methodical plan. Well-written standards and specifications can help vastly. The intentional development of AM alloys for specialized aerospace applications is expected to grow, but focus should be maintained to fully mature all aspects of the AM life cycle including property development and demonstration in the application environment. The outlook of AM alloy development for of extreme environments is very promising.

Author contributions

P.R.G. – Conceptualization, Methodology, Writing – Original Draft, Investigation, Resources; **O.R.M.** – Conceptualization, Methodology, Writing – Original Draft, Investigation, Resources; **C.K.** – Conceptualization, Methodology, Writing – Original Draft, Investigation; **T.M.S.** – Conceptualization, Methodology, Writing – Original Draft, Investigation; **J.S.** – Methodology, Writing – Original Draft, Investigation; **A.P.** – Methodology, Review & Editing; **P.S.C.** – Conceptualization, Methodology, Investigation, Review & Editing; **D.C.T.** – Review & Editing; **C.S.P.** – Conceptualization, Methodology, Investigation, Resources, Review & Editing; **T.W.T.** – Original Draft, Investigation; **D.L.E.** – Conceptualization, Methodology, Investigation, Review & Editing; **C.A.K.** –

Conceptualization, Methodology, Writing – Original Draft, Investigation.

Declaration of competing interest

The authors declare that they have no known competing financial interests or personal relationships that could have appeared to influence the work reported in this paper.

Acknowledgements

This research was funded by NASA under additive manufacturing development efforts through the Rapid Analysis and Manufacturing Propulsion Technology (RAMPT), Optimized and Repeatable Components using Additive (ORCA), Refractory Additive Alloy Manufacturing and Build Optimization (RAAMBO), and Transformational Tools and Technologies projects. This paper describes objective technical results and analysis. Any subjective views or opinions that might be expressed in the paper do not necessarily represent the views of the National Aeronautics and Space Administration (NASA) or the United States Government. The results from this study are solely for informational purposes and not an endorsement of any techniques by the authors, their employers, or the publishing journal.

The authors would like to thank various partners in the development and advancement of these various alloys including RPM Innovations, Tyler Blumenthal/RPMI, Launcher Space (Tim Berry, Max Haot, Andre Ivankovic), AME, Elementum 3D, Castheon (ADDMan), Powder Alloy Corp, Praxair, ATI, Noah Burchett, Declan Dink Murphy, Louisiana State University (LSU) for conductivity testing, Auburn University for characterization of NASA HR-1, WMTR, IMR Testing. There are also many individuals involved in the development of these alloys across NASA and industry – thank you. Thank you to Lynn Machamer for help with graphics and formatting.

Appendix A

Table A
Tensile properties of HIPed GRX-810 with respect to temperature.

Temp. (°C)	Tensile Strength (MPa)	Yield Strength (MPa)	Elong. (%)
-195.6	1227.3	723.9	49
21.1	848.1	515.0	43
426.7	655.0	410.2	40
648.9	630.9	368.9	43
871.1	262.7	206.2	62
1000.0	164.1	161.3	44
1093.3	119.3	115.8	32

References

- [1] B. Blakey-Milner, P. Gradi, G. Snedden, M. Brooks, J. Pitot, E. Lopez, et al., Metal additive manufacturing in aerospace: a review, Mater. Des. 209 (2021), 110008, <https://doi.org/10.1016/j.matdes.2021.110008>.
- [2] B.N. Bhat (Ed.), Aerospace Materials and Applications, American Institute of Aeronautics and Astronautics, Inc., Reston ,VA, 2018, <https://doi.org/10.2514/4.104893>.
- [3] P. Gradi, D. Tinker, A. Park, O. Mireles, M. Garcia, R. Wilkerson, et al., Robust metal additive manufacturing process selection and development for aerospace components, J. Mater. Eng. Perform. (2021), <https://doi.org/10.1007/s11665-022-06850-0>. Springer.
- [4] Paul R. Gradi, Omar R. Mireles, Christopher S. Protz, Chance P. Garcia, Metal Additive Manufacturing for Propulsion Applications, first ed., American Institute of Aeronautics and Astronautics, Inc., Reston, VA, 2022 <https://doi.org/10.2514/4.106279>.
- [5] P.R. Gradi, S.E. Greene, C. Protz, B. Bullard, J. Buzzell, C. Garcia, et al., Additive manufacturing of liquid rocket engine combustion devices: a summary of process developments and hot-fire testing results, in: 2018 Jt. Propuls. Conf., American Institute of Aeronautics and Astronautics Inc, AIAA, 2018, <https://doi.org/10.2514/6.2018-4625>.
- [6] P.R. Gradi, C.S. Protz, D.L. Ellis, S.E. Greene, Progress in additively manufactured copper-alloy GRCop-84, GRCop-42, and bimetallic combustion chambers for liquid rocket engines, Proc. Int. Astronaut. Congr. IAC 2019 October 21 (2019) 21–25.
- [7] P.R. Gradi, C.S. Protz, Technology advancements for channel wall nozzle manufacturing in liquid rocket engines, Acta Astronaut. 174 (2020), <https://doi.org/10.1016/j.actaastro.2020.04.067>.
- [8] T.M. Smith, A.C. Thompson, T.P. Gabb, C.L. Bowman, C.A. Kantzos, Efficient production of a high-performance dispersion strengthened, multi-principal element alloy, Sci Reports 2020 10 (101) (2020) 1–9, <https://doi.org/10.1038/s41598-020-66436-5>.
- [9] National Research Council (U.S. Committee on Integrated Computational Materials Engineering. Integrated Computational Materials Engineering : a Transformational Discipline for Improved Competitiveness and National Security, 2008, p. 137.
- [10] M. Seifi, A. Salem, J. Beuth, O. Harrysson, J.J. Lewandowski, Overview of materials qualification needs for metal additive manufacturing, J. Occup. Med. 68 (2016) 747–764, <https://doi.org/10.1007/s11837-015-1810-0>.
- [11] Song Q. song, Y. Zhang, Wei Y. feng, Zhou X. yi, Shen Y. fu, Y min Zhou, et al., Microstructure and mechanical performance of ODS superalloys manufactured by

- selective laser melting, Opt Laser. Technol. 144 (2021), 107423, <https://doi.org/10.1016/j.optlastec.2021.107423>.
- [12] F. Kerstens, A. Cervone, P. Gradl, End to end process evaluation for additively manufactured liquid rocket engine thrust chambers, Acta Astronaut. 182 (2021) 454–465, <https://doi.org/10.1016/j.actaastro.2021.02.034>.
- [13] R.P. Minneci, E.A. Lass, J.R. Bunn, H. Choo, C.J. Rawn, Copper-based alloys for structural high-heat-flux applications: a review of development, properties, and performance of Cu-rich Cu–Cr–Nb alloys, Int. Mater. Rev. (2020), <https://doi.org/10.1080/09506608.2020.1821485>.
- [14] J. Lee. Hydrogen embrittlement. NASA Technical Memorandum, 2016. NASA/TM-2016-218602, <https://ntrs.nasa.gov/citations/20160005654>. NASA/TM-2016-218602.
- [15] M. Li, S.J. Zinkle, Physical and mechanical properties of copper and copper alloys, Compr Nucl Mater 4 (2012) 667–690, <https://doi.org/10.1016/B978-0-08-056033-5.00122-1>.
- [16] H.C. DeGroh, D.L. Ellis, W.S. Loewenthal, Comparison of GRCop-84 to other Cu alloys with high thermal conductivities, J. Mater. Eng. Perform. 17 (2008) 594–606, <https://doi.org/10.1007/s11665-007-9175-3>.
- [17] P.R. Gradl, C. Protz, K. Cooper, C. Garcia, D. Ellis, L. Evans, GRCop-42 development and hot-fire testing using additive manufacturing powder bed fusion for channel-cooled combustion chambers, AIAA Propuls. Energy Forum Expo 2019 (2019), <https://doi.org/10.2514/6.2019-4228>. American Institute of Aeronautics and Astronautics Inc, AIAA.
- [18] J. Svoboda, V. Horník, L. Stratil, H. Hadraba, B. Mašek, O. Khalaj, et al., Microstructure evolution in ods alloys with a high-volume fraction of nano oxides, Metals 8 (2018), <https://doi.org/10.3390/met8121079>.
- [19] W.J. Quadakkers, H. Holzbrecher, K.G. Briefs, H. Beske, Differences in Growth Mechanisms of Oxide Scales Formed on ODS and Conventional Wrought Alloys, vol. 32, 1989.
- [20] T.M. Smith, C.A. Kantzios, N.A. Zarkevich, B.J. Harder, M. Heczko, P.R. Gradl, et al., A 3D printable alloy designed for extreme environments, Nature (2023), <https://doi.org/10.1038/s41586-023-05893-0>.
- [21] J. Wadsworth, T.G. Nieh, J.J. Stephens, Recent advances in aerospace refractory metal alloys 33 (2013) 131, <https://doi.org/10.1179/IMR.1988.33.1.131>, 50.
- [22] P.R. Gradl, S. Elam Greene, C.S. Protz, D.L. Ellis, B.A. Lerch, S.E. Greene, et al., Development and hot-fire testing of additively manufactured copper combustion chambers for liquid rocket engine applications, 53rd AIAA/SAE/ASEE Jt Propuls Conf 1–27 (2017), <https://doi.org/10.2514/6.2017-4670>.
- [23] Ogbuji Lu, D.L. Humphrey, J.A. Setlock, Oxidation-reduction resistance of advanced copper alloys August (2003).
- [24] Ogbuji Lu, D.L. Humphrey, Oxidation of Copper Alloy Candidates for Rocket Engine Applications, National Space and Missile Materials Symposium, Colorado Springs, CO, 2002.
- [25] D.L. Ellis, K. Taminger, C. Protz, J. Fikes, Low-Cost Upper Stage-Class Propulsion (LCUSP): Final Report, 2022.
- [26] Ellis DL, Loewenthal WS, Yun HM. Tensile Properties of GRCop-84. Nasa/Tm-2012-217108 2012.
- [27] T.W. Teasley, NASA Succeeds in Testing of Advanced Rotating Detonation Rocket Engine for New US Space Flight Capability, 2022.
- [28] P.R. Gradl, T.W. Teasley, C.S. Protz, M.B. Garcia, D. Ellis, C. Kantzios, Advancing GRCop-based bimetallic additive manufacturing to optimize component design and applications for liquid rocket engines, AIAA Propuls. Energy 2021 (2021) 1–28, <https://doi.org/10.2514/6.2021-3231>.
- [29] T. Teasley, B. Williams, A. Larkey, C. Protz, P. Gradl, A review towards the design optimization of high-performance additively manufactured rotating detonation rocket engine injectors, AIAA Propuls Energy Forum (2021 2021), <https://doi.org/10.2514/6.2021-3655>.
- [30] T.W. Teasley, T.M. Fedotowsky, P.R. Gradl, B.L. Austin, S.D. Heister, Current state of NASA continuously rotating detonation cycle engine development, AIAA Scitech 2023 (2023) 1–24, <https://doi.org/10.2514/6.2023-1873>. AIAA.
- [31] C. Katsarelis, P. Chen, P.R. Gradl, C. Protz, Z. Jones, N. Marshall, et al., Additive manufacturing of NASA HR-1 material for liquid rocket engine component applications, JANNAF Jt Propuls Conf (2019). <https://ntrs.nasa.gov/search.jsp?R=20200001007>.
- [32] P.S. Chen, C.C. Katsarelis, W.M. Medders, P.R. Gradl, Segregation Evolution and Diffusion of Titanium in Directed Energy Deposited, NASA Tech Memo. <https://ntrs.nasa.gov/citations/20210013649>.
- [33] P.R. Gradl, T.W. Teasley, C.S. Protz, C. Katsarelis, P. Chen, Process development and hot-fire testing of additively manufactured NASA HR-1 for liquid rocket engine applications, AIAA Propuls. Energy 2021 (2021) 1–23, <https://doi.org/10.2514/6.2021-3236>.
- [34] P.-S. Chen, M. Mitchell, Aerospace Structural Metals Handbook Alloy NASA-HR-1 Nickel Base Alloys-Ni, 2005.
- [35] P.S. Chen, C.C. Katsarelis, W.M. Medders, P.R. Gradl, C.H. Su, Development of directed energy deposited NASA HR-1 to optimize properties for liquid rocket engine applications, NASA Tech. Memo. NASA/TM-20230006075. ntrs.nasa.gov/20230006075.
- [36] A. Soltani-tehrani, P. Chen, C. Katsarelis, P. Gradl, S. Shao, Thin-Walled Structures Mechanical properties of laser powder directed energy deposited NASA HR-1 superalloy : effects of powder reuse and part orientation, Thin-Walled Struct. 185 (2023), 110636, <https://doi.org/10.1016/j.tws.2023.110636>.
- [37] P. Gradl, A. Cervone, P. Colonna, Integral Channel nozzles and heat exchangers using additive manufacturing directed energy deposition NASA HR-1 alloy, 73rd Int. Astronaut. Congr., Paris, France 2 (2022), x73690. IAC-22,C4.
- [38] Y. Brif, M. Thomas, I. Todd, The use of high-entropy alloys in additive manufacturing, Scripta Mater. 99 (2015) 93–96, <https://doi.org/10.1016/j.scriptamat.2014.11.037>.
- [39] S. Chen, Y. Tong, P.K. Liaw, Additive manufacturing of high-entropy alloys: a review, Entropy 20 (2018), <https://doi.org/10.3390/e20120937>.
- [40] F. Weng, Y. Chew, Z. Zhu, X. Yao, L. Wang, F.L. Ng, et al., Excellent combination of strength and ductility of CoCrNi medium entropy alloy fabricated by laser aided additive manufacturing, Addit. Manuf. 34 (2020), 101202, <https://doi.org/10.1016/j.addma.2020.101202>.
- [41] T.M. Smith, A.C. Thompson, T.P. Gabb, C.L. Bowman, C.A. Kantzios, Efficient production of a high-performance dispersion element alloy, Sci. Rep. (2020) 1–9, <https://doi.org/10.1038/s41598-020-66436-5>.
- [42] T.M. Smith, Additive Manufactured Alloys for HighTemperature Applications, NASA T2 Webinar, 2022.
- [43] O. Mireles, Additive manufacture of refractory metals for aerospace applications, AIAA Propuls. Energy 2020 Forum (2021) 1–9, <https://doi.org/10.2514/6.2021-3234>.
- [44] O.R. Mireles, O. Rodriguez, Y. Gao, N. Philips, Additive Manufacture of Refractory Alloy C103 for Propulsion Applications. AIAA Propuls. Energy 2020 Forum, American Institute of Aeronautics and Astronautics Inc, AIAA, 2020, pp. 1–13, <https://doi.org/10.2514/6.2020-3500>.
- [45] A. Talignani, R. Seede, A. Whitt, S. Zheng, J. Ye, I. Karaman, et al., A review on additive manufacturing of refractory tungsten and tungsten alloys, Addit. Manuf. 58 (2022), 103009, <https://doi.org/10.1016/J.ADDMA.2022.103009>.
- [46] P.D. Awasthi, P. Agrawal, R.S. Haridas, R.S. Mishra, M.T. Stawowy, S. Ohm, et al., Mechanical properties and microstructural characteristics of additively manufactured C103 niobium alloy, Mater. Sci. Eng., A 831 (2022), 142183, <https://doi.org/10.1016/J.MSEA.2021.142183>.
- [47] C.J. Romnes, J.F. Stubbins, O.R. Mireles, Tuning the properties of additively manufactured tungsten ultra-fine lattices by adjusting laser energy density and lattice geometry, J. Mater. Eng. Perform. (2022 2022) 1–14, <https://doi.org/10.1007/S11665-022-07126-3>.